https://dx.doi.org/10.22161/ijaers *ISSN: 2349-6495(P) | 2456-1908(O)*

Study on Modification of Lignin as Dispersant of Aqueous Graphene Suspension and Corrosion Performance in Waterborne G/Epoxy Coating

Jiheng Ding[1], Shubin Shi[1,2], Haibin Yu[1]

[1] Key Laboratory of Marine Materials and Related Technologies, Key Laboratory of Marine Materials and Protective Technologies of Zhejiang Province, Ningbo Institute of Materials Technology and Engineering, Chinese Academy of Sciences, Ningbo 315201, P. R. China；

[2] School of Materials, Shanghai University Shanghai 200444, P. R. China.

Abstract— *Though graphene (G) as an excellent protective material for metal, it can aggravate metal corrosion in other side. The modification of sodium lignin sulfonate was achieved by using itaconic acid and acrylamide，which was proved by UV-vis and Raman spectra. The modified sodium lignin sulfonate (LAI) with more carboxylic groups can be used as the dispersant for aqueous graphene suspension. The commercial graphene can be dispersed uniformly and stability in water via π-π interaction with LAI at high concentration (6 mg/mL)，and the LAI-G system can be used as an inhibitor in waterborne epoxy coatings too. Electrochemical impedance spectroscope (EIS) and Tafel polarization curves showed that the corrosion performance of waterborne epoxy system with well-dispersed G (0.5 wt %) was remarkably improved compared with pure epoxy coating.*

Keywords— sodium lignin sulfonate, graphene, waterborne epoxy coating, dispersion, corrosion resistance.

I. INTRODUCTION

Nowadays, waterborne coatings have gained more and more attention on metal protection on account of the strict regulations about the use of volatile organic compound (VOC). However, the anticorrosion performance of waterborne coating is farther inferior to the solvent one because the hydrophilic groups were retained in waterborne coating after the film formation, which decreases the shielding effects to water, oxygen and chlorine ions, et al. Considering the above reasons, it is necessary to add inhibitors or fillers into waterborne coatings to improve their corrosion resistance[1-5].

Graphene, a 2D layer of sp^2-hybridization single-atom-thick sheet, possesses remarkable mechanical inertness, thermal conductivity and impermeability to molecules, and so forth, it has been a useful material for metal protection in different fields. As we all know, CVD-graphene is a kind of superior anticorrosion film, but it has no effect on protecting metal for a long-term because of the film defects[6-11]. Generally, Oxidation-reduction and liquid-phase exfoliation are the most two effective methods for large scale-preparation of graphene-powder, however, it is very prone to aggregate together in solution, in consequence the application of graphene in the fields of anticorrosion coatings is greatly limited[12-14].

Usually, the preparation of aqueous graphene sheets could be summarized into two categories. The first method is chemical modification, which is to prepare well-water-soluble graphene via grafting-from or grafting-to approaches. However, this method tends to

induce defects or even destruction which can alter the inherent properties of graphene especially electrical properties and thermal conductivity. The other method is non-covalent fictionalization, which is based on van der Waals forces or π-π interactions between the surfactants and the sp^2 hybridized atoms of graphene, and it possesses higher efficiency and conservation for the properties of graphene than the former one[15-17]. For example, Lin et al. synthesized an aniline trimer derivative (CAT) by reaction of aniline trimer and anhydride, which could be used as a stabilizer to disperse commercial graphene in water stability at high concentration (generally, >1 mg/mL) via strong π-π interaction between the CAT and graphene[18]. Lijun et al. reported the preparation of the bio-based epoxy monomer gallic acid-based epoxy resin (GA-II) from tannic acid derivative and it was used as a novel surfactant or stabilizer for graphene suspension, which was capable of being absorbed onto the surface of graphene via strong π-π interactions，and could inhibits graphene aggregating and facilitate homogeneous dispersion in epoxy matrix[19].

Lignin is a kind of sustainable natural polymer，and it is widely found in wood and plant resources. Generally, Lignin is the by-product in paper industry, and it is always poured into rivers as a waste, which is not only a loss of energy, but also causes serious environment pollution. The development and high value utilization of lignin has become great both economic and social benefits. Lignin and its derivatives usually can be used as dispersant for dyes, pesticides and coals et, al. For example, Song et al, prepared a new dispersant for water coal slurry by using sodium lignosulphonate and itaconic acid, and the authors studied on the effects of the dosage of itaconic acid，the dosage of initiator，reaction time and reaction temperature on apparent viscosity of coal water slurry were examined[20]. As far as we know, there no literature on the preparation of lignin as the waterborne graphene dispersant for corrosion resistance on coatings. The modification of lignin can offer an alternative way for reutilization of the waste biomass resource and it is expected to be used as the dispersant for graphene[21-24].

In order to make better use of lignin resources and provides a theoretical basis for its performance improvement. In our present study, a lignin terpolymer (LAI) was prepared by taking the sodium lignosulphonate as a raw material, which was used as a dispersant of commercial graphene in water and then we prepared LAI-G/epoxy composite coatings. What we expect is that the LAI can play a dual role in the epoxy composites: (1) promoting the dispersion of commercial graphene in waterborne epoxy matrix, (2) serving as a inhibitor on the metal base[25-30].

II. EXPERIMENTAL

2.1 Materials

Sodium lignosulphonate (LS), itaconic acid (IA), acrylamide (AA) and ammonium persulfate were purchased from Aladdin Industrial Corporation, and were used without further purification. Graphene (length: 5～20 μm; layer thickness: 2～5 nm; layer number: 3～10; purity: 99.5%; water mass fraction: 93.8 wt%) was provided by Ningbo Morsh Technology. Co., Ltd and used without further purification. Deionized water was used throughout the experiment. Waterborne epoxy resin (EP-AB-W53) and waterborne curing agent (HGA-AB-20) were provided by Zhejiang business development of new materials. Co., Ltd. The Q235 carbon steel electrode was provided by OSS integral institute Co., Ltd. was selected for anticorrosion test. All other reagents were purchased from Aladdin and used as received and without other disposition.

2.2 Synthesis of lignin terpolymer (LAI)

1 g of LS, 0.035 g ammonium persulfate and 19 g of deionized water were added into four necked round-bottom flask of 250 mL, then the mixture was vigorously stirred at room temperature for 30 minutes until LS was completely dissolved. 4 g of itaconic acid and 4 g of acrylamide were dropped into the

above-mentioned solution at 75 °C for 4.5 h in a water bath under the nitrogen atmosphere. Then the solution was precipitated by isopropanol and the rough product was extracted with acetone for 8 h. Finally, the pure product was dried at 30 °C in a vacuum to achieve constant weight. Yield: ～85%.

2.3 Preparation of LAI functionalized waterborne graphene dispersant

Typically, 0.6 g of LAI was added into 100 mL water and then sonicated (200 W) for 10 min. The pH value of above solution was adjusted to 8-9 by NaOH aqueous. After that, 0.6 g of graphene was added into above solution and sonicated in a 650 W sonicator for 2 h to obtain a LAI-G hybrid dispersant after 30 days there is no obvious precipitates were observed.

2.4 Preparation of the LAI-G/epoxy composites

The LAI-G/epoxy composites were prepared by the following procedure: the obtained dispersion of LAI-G was added into waterborne epoxy coatings in accordance with 0.5 wt%, then the mixture was stirred magnetically for 10 min. The liquid of LAI-G/epoxy composites were coated on the surface of Q235 carbon steel electrode with a bar coater, the specimens were dried at room temperature and 60 °C for 12 h respectively. The film thickness was 25±2 μm measured using a PosiTector6000FNS1 apparatus. The pure epoxy coating was prepared in a similar way without any graphene addition.

2.5 Characterizations

The FTIR spectrum (KBr) was collected with a Thermo Nicolet Nexus 6700 instrument. The ultraviolet-visible (UV-vis) spectroscopy were obtained using a Lambda 950 UV-vis spectrometer. Raman spectra were recorded with a confocal Raman spectrometer (Renishaw invia Reflex) using the wavelength of 632.8 nm. Tapping mode atomic force microscopy (AFM) was conducted on a Dimension 3100V scanning probe microscope, and the samples were prepared by dropcasting the LAI-G dispersion on new cleaved mica surfaces. The morphology of graphene and its composites were investigated by a Tecnai G2 F20 transmission electron microscopy (TEM) at the accelerating voltage of 200 kV and a FEI Quanta FEG 250 scanning electron microscope (SEM) respectively.

The anticorrosion performances of coatings were performed on CHI-660E electrochemical workstation. The electrochemical impedance spectroscopy (EIS) and potentiodynamic polarization curves were acquired in 3.5wt% NaCl water solution using a classical three-electrode arrangement (the Q235 carbon steel electrode as a research electrode, saturated calomel electrode as a reference electrode and platinum electrode as an auxiliary electrode). Typically, the coating/Q235 steel specimen were initially kept at an open circuit potential (OCP) for 0.5 h before measurement, and the final corrosion parameters were fitted form EIS data using ZsimpWin 3.21 software. Polarization curves were performed with 0.5 mV/s scan rate and started from a potential of -250 mV to +250 mV vs.OCP.

III. RESULTS AND DISCUSSION

3.1 Synthesis and characterization of lignin terpolymer (LAI)

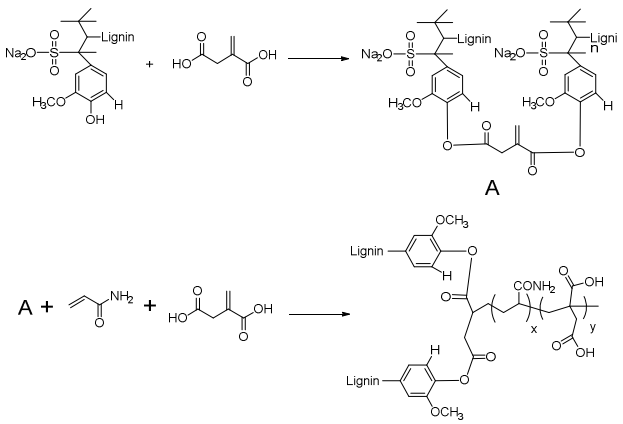

Scheme 1: Reaction route for the synthesis of lignin terpolymer (LAI).

The LAI was synthesized according to the scheme 1. The reaction mechanism of LA, IA and AA: first, the product A was obtained by the etherification of LS and partly IA; secondly, the final product LAI was obtained from the

https://dx.doi.org/10.22161/ijaers *ISSN: 2349-6495(P) | 2456-1908(O)*

polymerization of A, IA and AA. And the chemical structures of LS and LAI were firmed by FTIR in Fig 1.

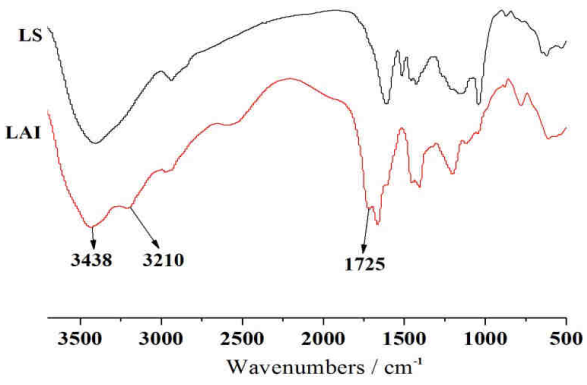

Fig.1: FTIR spectra of LS and LAI.

The FTIR spectra of LS and LAI samples in the wavelength range of 4000 to 400 cm^{-1} are showed in Fig 1, respectively. As shown in Fig 2-LS, the absorption peak at 3450 cm^{-1} is assigned to O-H and the peak (associative hydroxyl group) was covered by the strong peak of O=C-NH in the picture of LAI. The new absorption peaks at 3120 cm^{-1} and 1725 cm^{-1} are O=C-NH and O=C-O, respectively. And the deformation vibration absorption peaks at 1455 cm^{-1} belong to O=C-NH and N-H. The stretching vibration absorption peak of C-N appeared at 960 cm^{-1}. Besides, there was little change in the rest peaks of LAI compared with other peaks from LS,. This result proved that LS has been grafted with IA and AA.

3.2 Fabrication and characterization of waterborne graphene suspension

Here, we prepared high concentration (6 mg/mL) waterborne dispersions of graphene sheets by using a water-soluble lignin derivative (LAI) as surface agent and stabilizer. The stability of LAI-G dispersion and direct dispersion of graphene in water from one day to 30 days as are shown in Fig 2. As we can see from the picture, the LAI-G dispersion was much more stable and no obvious precipitates were observed (Fig 2 b). However, the direct dispersion of graphene without stabilizers resulted in sedimentation after 15days (Fig 2 a).

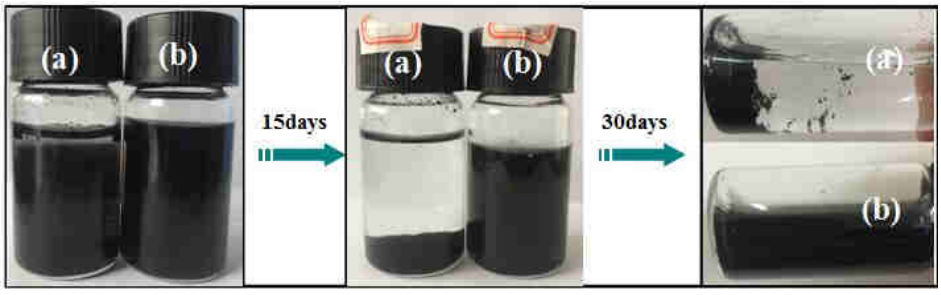

Fig.2: The stability of waterborne graphene dispersant

The Raman spectra of graphene and LAI-G system are shown in Fig 3, which indicates the π–π interaction between graphene and LAI. Graphene usually exhibits a G band at 1580 cm^{-1}, a D band at 1350 cm^{-1} and a 2D band at 2750 cm^{-1}on the Raman spectra. The G band is the characteristic peaks of C sp^2 atom structure, reflecting the symmetry and the degree of crystallization, the D band corresponds the breaking mode near the K zone boundary, and the 2D band is derived from two double phonon inelastic scattering. Obviously, the G band of LAI-G was red-shifted from 1587 cm^{-1} for graphene to 1584 cm^{-1}, providing that the evidence for a charge transfer between the graphene sheet and LAI molecule.

https://dx.doi.org/10.22161/ijaers *ISSN: 2349-6495(P) | 2456-1908(O)*

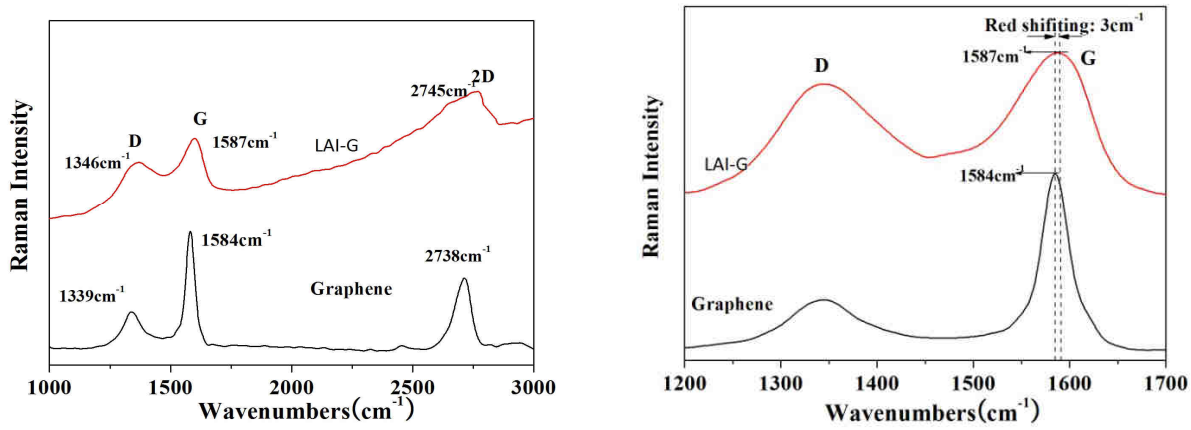

Fig 3. Raman spectra of graphene and LAI-G

In order to gain insight into the interaction between LAI and graphene sheets, the dispersion of LAI-G was studied by UV-vis spectrometer. The UV-vis spectra of LAI and LAI-G in water are shown in Fig 4. The absorption peak at 283 cm^{-1} was attributed to n-π* electron transition of LAI. To the dispersion of LAI-G, however, the peak for n-π* electron transition with a slight blue-shifted, which manifested that the π–π interaction between graphene and LAI.

The high concentration dispersion state of waterborne graphene sheets containing LAI were directly observed by atomic force microscopy (AFM) and transmission electron microscopy (TEM) in Fig 5. The size of the graphene sheets was about several micrometres and the average thickness was ～2.5 nm as can be observed, which proves that the graphene sheets were almost exfoliated. The nanolayer was a little thinner than single graphene, which might be due to the LAI molecules were absorbed on the surface of graphene. The Fig. 5a and 5b display typical TEM micrographs of pristine graphene sheets and graphene modified by LAI. The pristine graphene looks like a thin film with a wrinkled surface, however, the LAI-G system layer is more transparent than the former. Those results above proved that the agglomeration of commercial graphene in water was prevented by the anchored LAI chain.

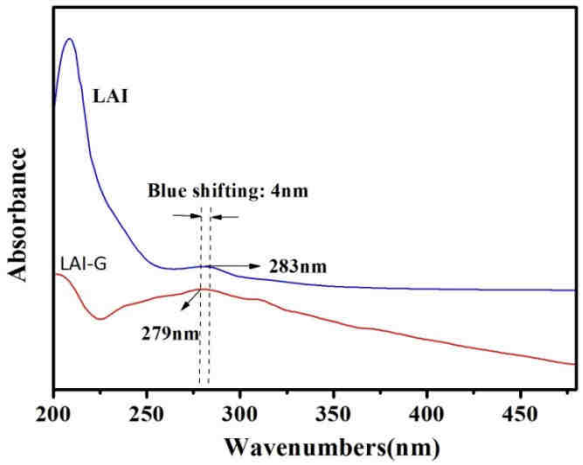

Fig 4: UV−vis spectra of LIA and LAI-G

https://dx.doi.org/10.22161/ijaers *ISSN: 2349-6495(P) | 2456-1908(O)*

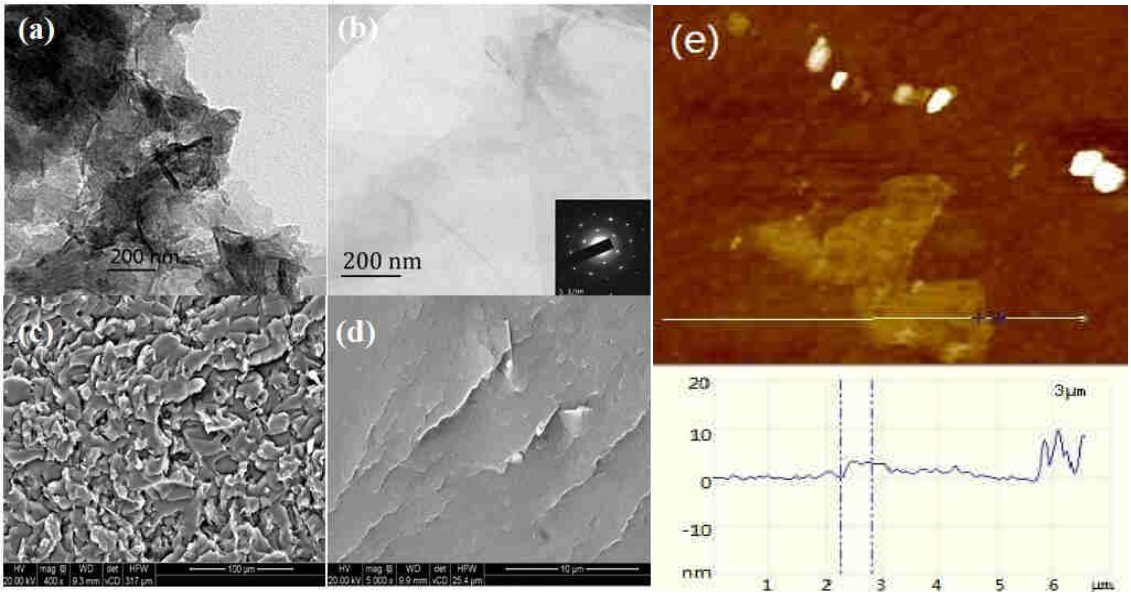

Fig.5:TEM images of pristine graphene (a) and LAI-G (b) from the solution suspension, typical SEM images for the LAI-G dispersed in epoxy matrix (c and d), and AFM image of LAI-G (e)

3.3 Morphologies of the LAI-G/epoxy composite

LAI-G/epoxy composites were prepared by two-component waterborne epoxy coating containing LAI and the dispersion capability of graphene sheets in the epoxy matrix was determined by SEM. Fig 5c and 5d show the fracture surface of graphene/epoxy composite containing 0.5 wt% LAI polymer under lower solution and high resolution, respectively. It can be seen that the diameter of graphene sheets is about 10 µm and well dispersed without any aggregation, and the graphene exhibited 2D parallel alignment in the epoxy matrix. The results noted above illustrates that the commercial graphene may be expected to play an important role in increasing the barrier effect and compactness of waterborne epoxy coating.

3.4 Anticorrosion properties of LAI-G/ epoxy coatings

In order to get stable potentials the OCP of different coatings were recorded every 12 h before testing the polarization and EIS curves. the OCP curves of different coatings in 3.5 wt% NaCl solution during the 96 h are shown Fig 6. The OCP values of two coatings appeared decrease during the first 24 h, and then remained stable. It can be seen from the curves, the OCP value of LAI-G/epoxy system was always more positive than the pure epoxy coating with time during whole the 96 h in immersion (the OCP values of pure and LAI-G/epoxy coatings are approximately -0.585V and -0.545 V after 24 h, and the values are remained -0.620 V and -0.582 V after 96 h). This result proves that the epoxy coating with LAI-graphene may improve the corrosion resistance of metal than the pure epoxy coating.

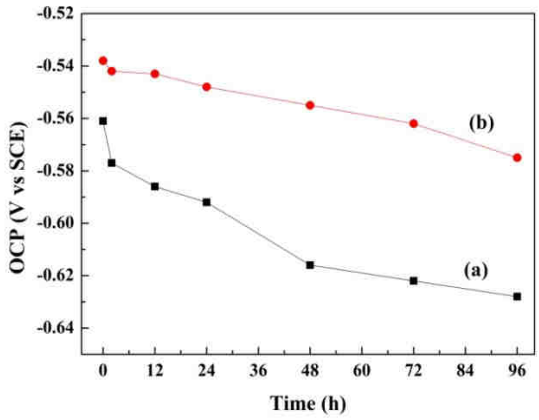

Fig 6: OCP curves for (a) LAI-G/epoxy , (b) pure epoxy coated electrode immersed in 3.5wt% NaCl solution after 96 h.

https://dx.doi.org/10.22161/ijaers *ISSN: 2349-6495(P) | 2456-1908(O)*

The anticorrosion behaviours of LAI-G/epoxy coatings were evaluated by the tafel polarization test and electrochemical impedance spectroscope (EIS). Fig 7 shows the anodic and cathodic polarization curves of pure epoxy and LAI-G/ (0.5 wt%) epoxy-coated on Q235 steel immersed in 3.5wt% NaCl solution at room temperature after 96 h. The corrosion density (i_{corr}), corrosion current potential (E_{corr}), anodic tafel slope (b_c) and cathodic tafel slope (b_a) were fitted from the extrapolation of the tafel zone and then marked in the graph.

$$P_{EF}\% = \frac{i_0 - i}{i_0}100\% \qquad (1\text{-}1)$$

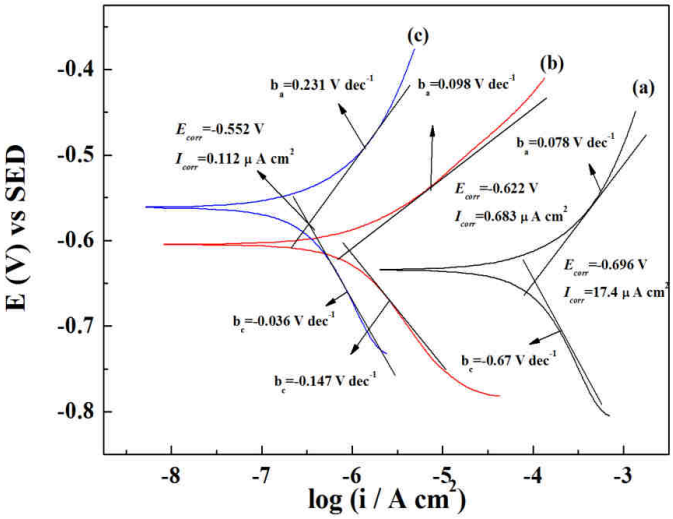

Fig. 7: Polarization curves for (a) bare steel , (b) pure epoxy and (c) LAI-G/epoxy coated electrode immersed in 3.5wt% NaCl solution after 96 h.

Generally, a higher E_{corr} and a lower i_{corr} reflect better corrosion protection. It can be seen that the E_{corr} = -0.552 V for LAI-G/epoxy coating is more positive than E_{corr} =-0.622 V for pure epoxy-coated and bare steel samples. In addition, the i_{corr} value (0.112 μA cm^{-2}) of the LAI-G/ epoxy coating was much lower than pure epoxy coating (0.683 μA cm^{-2}) and bare steel (17.4 μA cm^{-2}). Besides, compared with pure epoxy coating, the b_a values (0.231 V dec^{-1} > 0.128 V dec^{-1}) of LAI-G/ epoxy coating was enhanced greatly, implying the anodic reaction was inhibited by the graphene. The protection efficiency of coatings were calculated from Eq (1-1), where i_0 and i are the corrosion current densities of bare steel coated specimens and, and the tafel parameters were listed Table 1. The protection efficiency of LAI-G/epoxy system was 99.4%, which was higher than 96.1% for pure epoxy system.

The above results prove that the well-dispersed graphene increases the tortuosity of the diffusion pathways of the corrosive species such as water, oxygen and chloride ions in the coatings and improved dramatically the corrosion resistance of epoxy coatings.

Table.1: The tafel parameters of bare steel and epoxy systems

Name	E_{corr} / v	i_{corr} /μA cm^{-2}	b_a /V dec^{-1}	b_a /V dec^{-1}	P_{EF}/%
Bare steel	-0.696	17.4	0.078	-0.67	-
Pure epoxy	-0.622	0.683	0.128	-0.147	96.1
LAI-G/epoxy	-0.552	0.112	0.231	-0.036	99.4

In order to further investigate the corrosion protection mechanism of LAI-G/ epoxy coatings, as the most intensive and nondestructive testing techniques for investigation and prediction of the organic coating in aqueous solution, EIS was employed to evaluate the degradation processes of various samples immersed in 3.5wt% NaCl solution after different times as shown in Fig 8.

According to Lin et al., the impedance modulus at 10^{-2} Hz ($|Z|_{0.01Hz}$) represents the ability of coatings to impede the flow of current between anodic and cathodic areas, which is inversely proportional to corrosion rate. The $|Z|_{0.01Hz}$ of pure epoxy coating in the initial 2 h immersion was 3.5×10^4 Ω cm^2, and this value dropped gradually to 1×10^4 Ω cm^2 after 96 h (Fig 7 (a) Bode). For the LAI-G/epoxy coating, the impedance modulus at $|Z|_{0.01Hz}$ decreased gradually from 3.5×10^5 Ω cm^2 to 2.5×10^8 Ω cm^2 after 48 h,

and then remained at this level (Fig 8 (b) Bode). It can be seen that the impedance modulus of LAI-G/epoxy coating was about one order higher than pure epoxy during the whole immersion times. This result proves that the anticorrosion performance of LAI-G/epoxy coating was more excellent than the pure epoxy coating without any graphene.

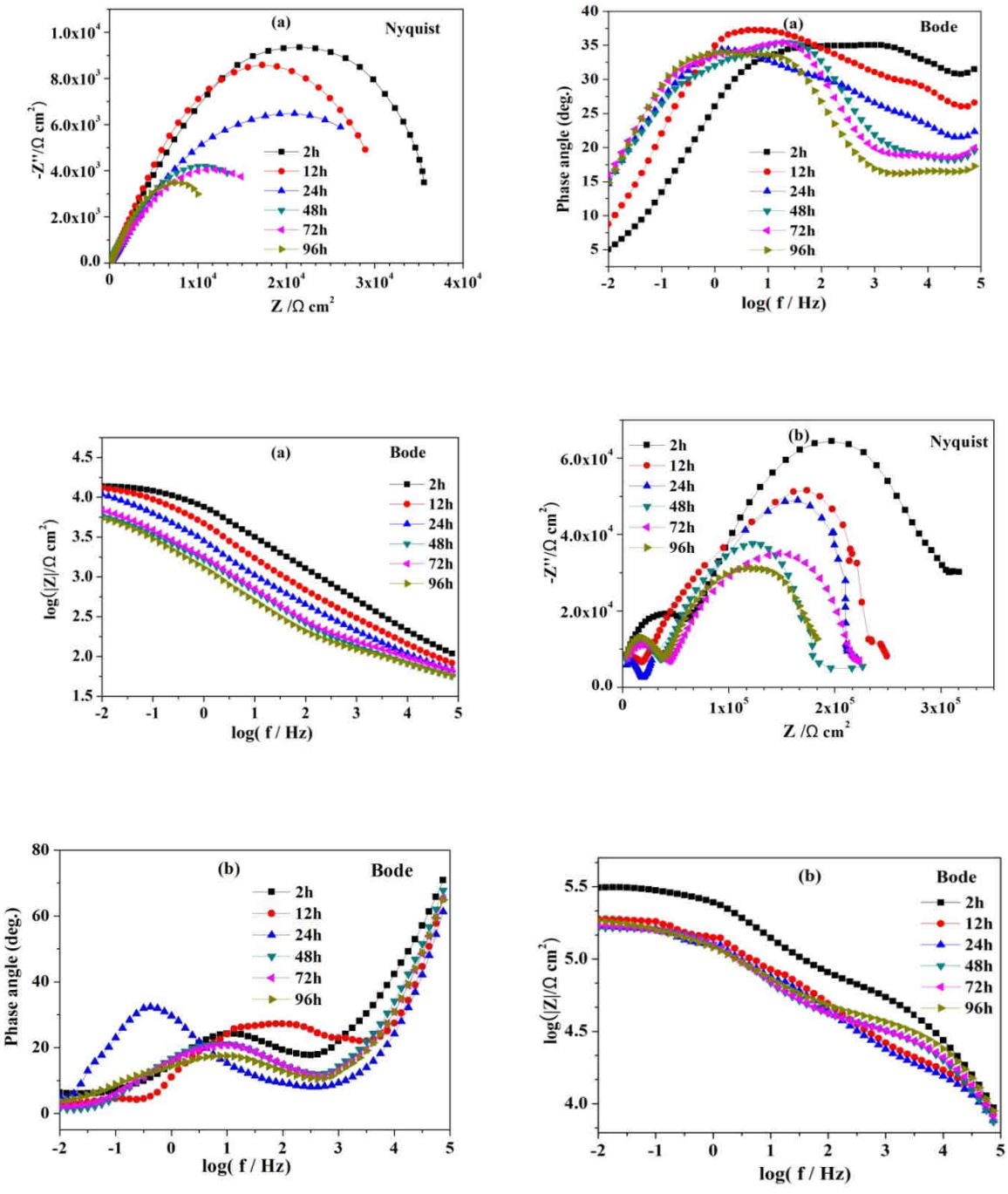

Fig.8: EIS curves of epoxy coatings:(a) pure epoxy and (b) LAI-G epoxy coated electrode immersed in 3.5% NaCl solution.

https://dx.doi.org/10.22161/ijaers *ISSN: 2349-6495(P) | 2456-1908(O)*

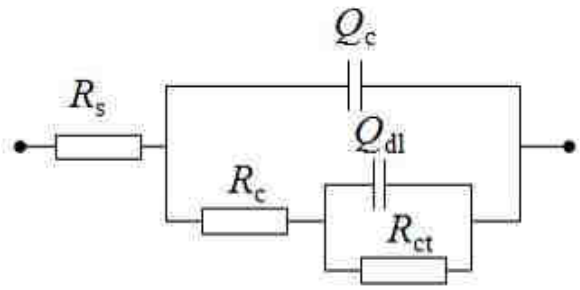

Fig.9: Equivalent circuit used to fit the EIS date.

Table.2: Electrochemical corrosion parameters fitted from the equivalent circuit

Samples	Time/ h	R_s/Ω cm^2	Q_c / μF cm^{-2}	n_1	R_c/KΩ cm^2	Q_{dl}/ μF cm^{-2}	n_2	R_{ct}/KΩ cm^2
pure epoxy	2	0.01	11.5	0.51	5.37	3.37	0.61	35.9
	12	0.01	18.2	0.51	0.920	17.3	0.55	33.5
	24	0.01	36.3	0.50	0.463	42.7	0.50	32.0
	48	0.01	94.1	0.50	0.275	26.5	0.63	25.9
	72	0.01	99.5	0.56	0.301	39.3	0.61	25.5
	96	0.01	176	0.58	0.190	95.1	0.52	17.8
G/LAI epoxy	2	0.01	0.0073	0.73	54.8	0.887	0.57	284
	12	0.01	0.0101	0.83	19.7	0.733	0.59	241
	24	0.01	0.0224	0.74	19.5	5.43	0.54	203
	48	0.01	0.0453	0.75	24.5	1.47	0.55	194
	72	0.01	0.223	0.72	26.1	1.87	0.55	186
	96	0.01	0.371	0.84	32.1	2.72	0.54	170

For quantitative estimate protection properties of LAI-G/epoxy and pure epoxy coatings, EIS parameters were fitted by using an equivalent circuits as shown in Fig 9, the corrosion parameters were listed in Table 2. The R_s, R_c and R_{ct} represent the solution resistance, coating resistance and charge-transfer resistance, respectively. Generally, R_c mainly depends on the amount of water uptake, and the higher R_c implies the smaller quantities of water, oxygen and chloride ions into the coatings. The R_{ct} is proportion to the corrosion rate and can be used to characterize the resistance to electron transfer across metal. Q_c and Q_{dl} represent the coating capacitance and double-layer capacitance, respectively [31].

Table 2 shows the immersion time dependence of R_c and R_{ct} for epoxy coatings. The R_c value of LAI-G/epoxy system decreased from 5.48×10^4 to 1.97×10^4 Ω cm^2 during 24 h of immersion. After 24 h immersion, the R_c value fluctuated and stabilized at 3.21×10^4 Ω cm^2. The higher R_c value should be owed to the increasing coverage areas of LAI on the metal surface and the coating plastic caused by the permeation of water. However, the coating resistance of pure epoxy coating without any graphene decreased dramatically from 0.54×10^4 to 0.19×10^3 Ω cm^2 during 96 h of immersion. Obviously, the R_c values of LAI-G/epoxy coating were much higher than pure epoxy coating during the whole immersion times. Moreover, the charge transfer

resistances R_{ct} implied the resistance of the electron transfer across the metal surface. The R_{ct} values of LAI-G/epoxy coating decreased from 2.84×10^5 to 1.70×10^4 Ω cm^2 during 96 h of immersion. The R_{ct} values of LAI-G/epoxy coating decreased from 3.59×10^4 to 1.78×10^4 Ω cm^2 during 96 h of immersion. The higher R_{ct} value of LAI-G/epoxy coating than pure epoxy coating indicates that LAI-G/epoxy coating has an more excellent barrier property on metal.

As the variation of dielectric constant the water uptake of different metal/coating systems were calculated based on the changes of the capacitances. And the water diffusion coefficient D could be obtained by means of the simplified Fick's second law of diffusion (Eq 1-2).

$$\frac{\lg Q_c - \lg Q_0}{\lg Q_\infty - \lg Q_0} = \frac{2}{L}\sqrt{\frac{D}{\pi}}\sqrt{t} \qquad (1\text{-}2)$$

Where Q_0, Q_c and Q_∞ are the coating capacitances at the beginning of the immersion time t_0, the time t_c and the time in saturated water absorption state t_∞, respectively. L is the coating thickness and D is the diffusion coefficient. The D of LAI-G/epoxy coating was calculated to be 1.27×10^{-9} cm^2/s , which was about one fifth of 5.78×10^{-9} cm^2/s for the pure epoxy coating. These results suggest that LAI-G/epoxy system showed better barrier property than pure epoxy.

3.5 Effect of LAI-G/epoxy matrix on the corrosion protection of the coating

There are two reasons to the results according to the analysed, and the anticorrosion mechanism were shown in the Fig 10. First, it may be ascribed to the good barrier and hydrophobic property of well-dispersed graphene in epoxy matrix. Secondly, the N^+ in LAI polymer was adsorbed on the metal surface by electrostatic interaction, which prevents the H^+ from further approaching the metal. And the N, O and other atoms in LAI have non-shared electron pairs, and they could form the coordination bond with the d orbital of the metal space, and a large number of groups containing N, O and other atoms attached to the surface of metal, and the space network structure of LAI macromolecular stretched into the internal of solution, which prevent water from approaching the metal surface, the LAI polymer played the role of corrosion inhibitor.

$$2Fe^{3+} + O + 2H^+ \longrightarrow 2Fe^{3+} + H_2O$$
(dissolved oxygen)

$$Fe^{3+} + LAI \rightleftharpoons Fe^{3+}[LAI]$$

(1-3)

Besides, the phenolic hydroxyl groups, alcohol phenolic hydroxyl groups, ether bonds and amide groups in the LAI structure could be formed complax with Fe^{3+} on the surface of metal, which has a shielding effect for ions. Therefore, the LAI-G/epoxy system shows higher corrosion resistance than the pure epoxy coating.

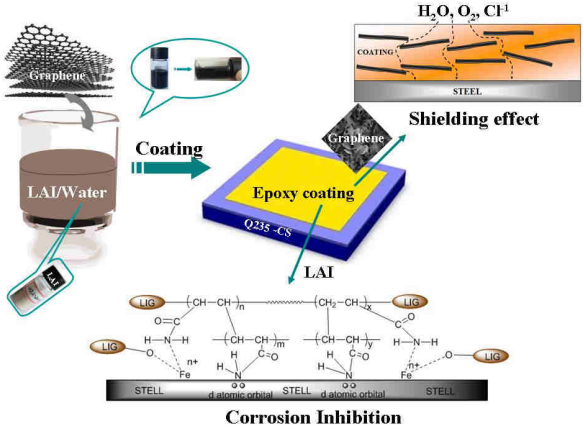

Fig.10: Schematic diagram of the anticorrosion mechanism of graphene and LAI ploymer.

IV. CONCLUSIONS

In this study, a bio-based agent LAI for commercial graphene dispersion was synthesized from renewable lignin and characterized using various spectroscopic methods. The increase of carboxyl and amide groups in lignin structure improved its water solubility, which can be a waterborne dispersant to inhibit aggregation and facilitate homogeneous dispersion of commercial graphene in waterborne epoxy coating. The corrosion protection properties and mechanism of epoxy coating

with graphene to carbon steel in 3.5% salt water were studied. The bio-based dispersant not only stably dispersed graphene at high concentration (～6 mg/mL) to almost 30 days, but also remarkably improved the corrosion protection of epoxy coating (the EIS exhibited the maximum inhibition efficiency of 99.4%). Moreover, the LAI could be synthesized through a green method.

ACKNOWLEDGEMENTS

The research is financially supported by the National Natural Science Foundation of China (Grant no. 21404112), China Postdoctoral Science Foundation (Grant no. 2014M561798) and Ningbo Natural Science Foundation (Grant no. 2015A610016). The authors thank Dr. Qing-Yun Wu in Ningbo University for her suggestion and discussion.

REFERENCES

[1] Gu, L.; Liu, S.; Zhao, H. C.; Yu, H. B., Anticorrosive Oligoaniline-containing Electroactive Siliceous Hybrid Materials. *RSC Adv. 69* **(2015)** 56011-56019.

[2] Liu, S.; Sun, H. Y.;, Sun, L. J., Effects of pH and Cl- concentration on corrosion behavior of the galvanized steel in simulated rust layer solution. *Corrosion Science*, 65（**2012**）520-527.

[3] Ding, J. H.; Zhao, H. R.; Gu, L.; Su, S. P.; Yu, H. B.; Epoxidation Modification of Renewable Lignin to Improve the Corrosion Performance of Epoxy Coating. *Int. J. Electrochem. Sci.*, 11 **(2016)** 6256 – 6265.

[4] Qiu, X.; Kong, Q.; Zhou, M.; Yang, D., Aggregation Behavior of Sodium Lignosulfonate in Water Solution. *J. Phys. Chem. B*, 114(2010),15857 – 15861.

[5] Liu, S.; Gu, L.; Zhao, H. C.; Yu, H. B., Corrosion Resistance of Graphene-Reinforced Waterborne Epoxy Coatings. *Journal of Materials Science & Technology*. 32 (**2016)**, 425–431.

[6] Gan, L. H.; Zhou, M. S.; Tian, S.; Yang, D. J.; Qiu, X. Q., Preparation and Evaluation of Carboxymethylated Lignin as Dispersant for Aqueous Graphite Suspension Using Turbiscan Lab Analyzer. *Journal of Dispersion Science and Technology.* 34 (**2013)**, 644–650.

[7] Zhang, C.; Huang, S.; Tjiu, W. W.; Fan, W.; Liu, T., Facile Preparation of Water-dispersible Graphene Sheets Stabilized by Acid-treated Multi-walled Carbon Nanotubes and their Poly(vinyl alcohol) Composites. *J. Mater. Chem.* 22 (**2012)**, 2427-2434.

[8] Gan, L. H.; Zhou, M. S.; Tian, S.; Yang, D. J.; Qiu, X. Q., Aggregation and adsorption behaviors of carboxymethylated lignin (CML) in aqueous solution.*Iran Polym J*. 23 **(2014)**, 47–52.

[9] Teng, C.-C.; Ma, C.-C. M.; Lu, C.-H.; Yang, S.-Y.; Lee, S.-H.; Hsiao, M.-C.; Yen, M.-Y.; Chiou, K.-C.; Lee, T.-M., Thermal Conductivity and Structure of Non-covalent Functionalized Graphene/Epoxy Composites. *Carbon*,49 *(***2011),** , 5107-5116.

[10] Cerrutti. B.; Souza, C.; Castellan, A.; Ruggiero, R., Frollini E Carboxymethyl lignin as Stabilizing Agent in Aqueous Ceramic Suspensions. *Ind Crops Prod*, 36 (2012),108–115.

[11] Cao, L.; Liu, X.; Na, H.; Wu, Y.; Zheng, W.; Zhu, J., How a Bio-based Epoxy Monomer Enhanced the Properties of Diglycidyl Ether of Bisphenol A (DGEBA)/Graphene Composites. *J. Mater. Chem. A* **, 16** (2013), 5081-5088.

[12] Deng, Y.; Feng, X.; Zhou, M.; Qian, Y.; Yu, H.; Qiu X.,Investigation of Aggregation and Assembly of Alkali Lignin Using Iodine As A Probe. *Biomacromolecules*, 12 (2011),1116–1125.

[13] Wang, J.; Somasundaran, P.; Nagaraj, D., Adsorption Mechanism of Guar Gum at Solid-Liquid Interfaces. *Miner Eng*, 18 (2005),77–81.

[14] Liu, Q.; Zhang, Y.; Laskowski, J., The adsorption of polysaccharides onto mineral surfaces: an acid/base interaction. *Int JMiner Process*, 60 (2000) ,229–245.

[15] Lee, J. H.; Choi, Y. M.; Paik, U.; Park, J. G., The Effect of Carboxymethyl Cellulose Swelling on The Stability of Natural Graphiteparticulates in An

Aqueous Medium for Lithium Ion Battery Anodes. *J Electroceram* ,17 (2006), 657–660.

[16] Li, J .,Advanced Analytical Chemistry. *Metallurgical Industry Press*, (2007), Beijing

[17] 17. Gu, L.; Liu, S.; Zhao, H. C.; Yu, H. B., Facile Preparation of Water-Dispersible Graphene Sheets Stabilized by Carboxylated Oligoanilines and Their Anticorrosion Coatings. *ACS Appl. Mater. Interfaces*, 7, (2015), 17641−17648.

[18] Cao, L. J.; Liu, X. Q.; Na, H. N.; Wu, Y. G.; Zheng, W. G.; Zhu, J.; How a bio-based epoxy monomer enhanced the properties of diglycidyl ether of bisphenol A (DGEBA)/graphene composites. *J Mater. Chem. A*, 1 (**2013)**, , 5081–5088.

[19] Song, J. W.; Guo, R.; Liu, J. B.; Wang, B. T., Characterization and Preparation of Copolymer of Itaconic Acid and Lignosulphonate. *Applied Chemical Industry*, 44 (2015), 559 – 662.

[20] Dutta, P.; Dey, J.; Ghosh, G.; Nayak, R. R., Self-association and Microenvironment of Random Amphiphilic Copolymers of Sodium *N*-acryloyl-l-valinate and *N*-dodecylacrylamide in Aqueous Solution. *Polymer*, 50 (2009) ,1516 – 1525.

[21] Binh-Khiem, N.; Matsumoto, K.; Shimoyama, I. Polymer Thin Film Deposited on Liquid for Varifocal Encapsulated Liquid Lenses. *Appl. Phys. Lett*, 93 (2008), 124101.

[22] Chen, C.-H.; Tsai, S.-L.; Chen, M.-K.; Jang, L.-S. Effects of Gap Height, Applied Frequency, and Fluid Conductivity on Minimum Actuation Voltage of Electrowetting-on-dielectric and Liquid Dielectrophoresis. *Sens. Actuators, B*, 159 (2011), 321−327.

[23] Li, X.; Cai, W.; An, J.; Kim, S.; Nah, J.; Yang, D.; Piner, R.; Velamakanni, A.; Jung, I.; Tutuc, E. Large-area Synthesis of Highquality and Uniform Graphene Films on Copper Foils. *Science*, 324 (2009), 1312−1314.

[24] Krupenkin, T.; Yang, S.; Mach, P. Tunable Liquid Microlens. *Appl. Phys. Lett.*, 82 (2003), 316−318.

[25] Lee, H.; Dellatore, S. M.; Miller, W. M.; Messersmith, P. B. Mussel-Inspired Surface Chemistry for Multifunctional Coatings. *Science*, 318 (2007), 426−430.

[26] Jin, X.; Zhou, W.; Zhang, S.; Chen, G. Z. Nanoscale Microelectrochemical Cells on Carbon Nanotubes. *Small*, 3(2007),1513−1517.

[27] Chao, D.; Zhu, C.; Xia, X.; Liu, J.; Zhang, X.; Wang, J.; Liang, P.; Lin, J.; Zhang, H.; Shen, Z. X.; Fan, H. J. Graphene Quantum Dots Coated VO2 Arrays for Highly Durable Electrodes for Li and Na Ion Batteries. *Nano Lett*, 15 (2015), 565−573.

[28] Yu, G.; Hu, L.; Liu, N.; Wang, H.; Vosgueritchian, M.; Yang, Y.; Cui, Y.; Bao, Z. Enhancing the Supercapacitor Performance of Graphene/MnO2 Nanostructured Electrodes by Conductive Wrapping. *Nano Lett*, 11(2011), 4438−4442.

[29] Merkel, T. C.; Lin, H. Q.; Wei, X. T.; Baker, R. Power plant postcombustion carbon dioxide capture: an opportunity for membranes. *J.Membr. Sci*, 359(2010), 126−139.

[30] Venna, S. R.; Carreon, M. A. Highly Permeable Zeolite Imidazolate Framework-8 Membranes for CO_2/CH_4 Separation. *J. Am. Chem. Soc*, 132 (2010), 76−78.

[31] Wind, M. M.; Lenderink, H. J. W., A Capacitance Study of Pseudo-fickian Diffusion in Glassy Polymer Coatings. *Prog. Org. Coat.* **1996,** *28* (4), 239-250.